

## Estudio de la fisuración en losa canal de mortero armado para uso en entresijos de vivienda.

### Study of cracking in reinforced mortar channel slabs for use in residential floors.

Ing. Gabriel Martínez Licea<sup>1</sup>, Dra. Isel del Carmen Díaz Pérez<sup>2</sup>, Dr. Hugo Wainshtok Rivas<sup>3</sup>

<sup>1</sup>Universidad Tecnológica de La Habana CUJAE, Calle 114 No. 11901 entre 119 y 127 Marianao, La Habana, Cuba

<sup>2</sup>Universidad Tecnológica de La Habana CUJAE, Calle 114 No. 11901 entre 119 y 127 Marianao, La Habana, Cuba

<sup>3</sup>Universidad Tecnológica de La Habana CUJAE, Calle 114 No. 11901 entre 119 y 127 Marianao, La Habana, Cuba

\*Autor de correspondencia: gabrielmarlic@civil.cujae.edu.cu

#### Resumen

La importancia del criterio de fisuración en los materiales cementicios o mortero armado, unido al insuficiente estudio experimental de elementos laminares de sección transversal canal reforzados con barras y malla(s) de alambres de acero, evidencian la necesidad de realizar más investigaciones en este sentido. Entre los principales factores que influyen en la fisuración se encuentra aquellos relativos al refuerzo, sin embargo, en la actualidad no se ha identificado un estudio sobre la disposición geométrica óptima del refuerzo con malla(s) en este tipo de elementos, en función de garantizar el cumplimiento del estado límite de fisuración, lo cual constituye el propósito de este trabajo. El estudio se realiza en losas canales considerando su uso en entresijos de viviendas. Para la obtención de la abertura máxima de fisura se emplea la expresión semiempírica desarrollada por Desayi y Ganesan y la resistencia a flexión se estima a partir de un modelo computacional calibrado con los ensayos experimentales realizados por estos investigadores. Los resultados demuestran que para cumplir con el ancho máximo de fisura permisible indicado por la norma ACI 549 1R-18, es obligatorio el empleo de malla(s) para el refuerzo de estos elementos. Además, se recomiendan valores mínimos de superficie específica y factor de volumen que debe(n) garantizar la(s) malla(s) para el refuerzo de los elementos de entresijos con las características analizadas.

**Palabras clave:** fisuración, mallas de acero, mortero armado, sección canal.

#### Abstract

The importance of the cracking criterion in cementitious materials or reinforced mortar, together with the insufficient experimental study of channel cross-section laminar elements reinforced with bars and wire mesh(es) of steel, show the need to carry out more research in this regard. Among the main factors that influence cracking are those related to reinforcement, however, at present no study has been identified on the optimal geometric arrangement of the reinforcement with mesh(es) in this type of elements, in order to guarantee compliance with the cracking limit state, which is the purpose of this work. The study is carried out on channel slabs considering their use in residential floors. To obtain the maximum crack opening, the semi-empirical expression developed by Desayi and Ganesan is used and the flexural strength is estimated from a computational model calibrated with the experimental tests carried out by these researchers. The results show that in order to comply with the maximum permissible crack width indicated by the ACI 549 1R-18 standard, the use of mesh(es) for the reinforcement of these elements is mandatory. In addition, minimum values

of specific surface area and volume factor are recommended that the mesh(es) must guarantee for the reinforcement of floor elements with the characteristics analyzed.

**Keywords:** Cracking, steel mesh, reinforced mortar, channel section.

## 1. Introduction

The degree of cracking of cementitious materials reinforced with steel bars and wires marks to a great extent the durability and aesthetics of a structure. These materials can be used in the conformation of prefabricated laminar or thin-walled elements, and be molded in different shapes and cross-sections, being the ribbed slab of channel section ( $\cap$ ) one of the most used rational shapes in housing mezzanines [1]. The low volume of these elements makes it possible to save cement and non-renewable resources and decreases the total load of the buildings. However, the restrictions indicated for reinforced mortar, as they are also called, are more stringent than reinforced concrete due to the small net cover of the reinforcement, which implies that the design is mainly governed by the cracking serviceability limit state [2].

The study of cracking in quasi-brittle materials is a challenge even today [3-12]. The verification of the maximum crack width or width is the most widespread method used in the current standards for the verification of this state, for this reason, most of the research on the subject are focused on obtaining this parameter. The ACI 549 1R-18 standard, corresponding to the design guide for ferrocement, limits the crack width for areas of medium or low aggressiveness to 0.10 mm, due to the small concrete cover and thin thickness of the element.

There are many factors that can affect cracking, although in general there is agreement that the most important factors are: the tension in the steel, the adhesion between the concrete and the steel, the amount of the main reinforcement, the diameter of the bars and their placement, the quality of the concrete and the height of the element. Bayu *et al.* [3] investigated the effect of the height of solid reinforced concrete slabs working in one direction and determined that this factor has a significant effect on the maximum crack width. Abu *et al.* [12] made a comparison between results from a computational model and the standard expressions for predicting maximum crack width in reinforced concrete beams, where they obtained that the reinforcing steel tension is the most influential factor together with the reinforcing steel characteristics: bar diameter, spacing, surface geometry and concrete cover.

In the literature there is scarce information on structural test results of channel slabs  $\cap$  of reinforced mortar, so their study is limited. To date, only the experimental re-search organized by Desayi and Ganesan [13], in which a semiempirical expression is developed to predict the maximum crack width in this type of  $\cap$  elements, could be identified.

The galvanized steel wire mesh, which is generally used as reinforcement of the reinforced mortar with the objective of controlling its cracking, constitutes its most expensive component. At the same time, an inadequate arrangement of the wires that form it and an excessive amount of meshes, hinder the compactness of the sand and cement matrix, which affects the quality of the panel. Likewise, it is favorable that the element is designed with the smallest possible height to reduce material consumption, decrease the weight of the elements, and to increase the probability that the mortar penetrates well into the end of the ribs in the manufacturing process [1].

Given the previous approaches, the objective of this work is to evaluate the influence of the geometric arrangement of the steel wire mesh (spacing and number of meshes, wire diameter) on the maximum crack width value in channel section reinforced mortar slabs, by means of the semi-

empirical expression developed by Desayi and Ganesan [13]. In addition, it aims to obtain the optimal arrangement of reinforcement meshes with respect to the cracking criterion, for use in residential floors.

## 2. Materials and Methods

The method developed by Desayi and Ganesan [13] to determine the maximum crack width in reinforced mortar channel slabs is based on the force balance of a reinforced concrete section, where the contribution of the bond strength of the reinforcing bar or wire is equalized to the axial force that generates the first crack in the effective area of the concrete (Fig 1).

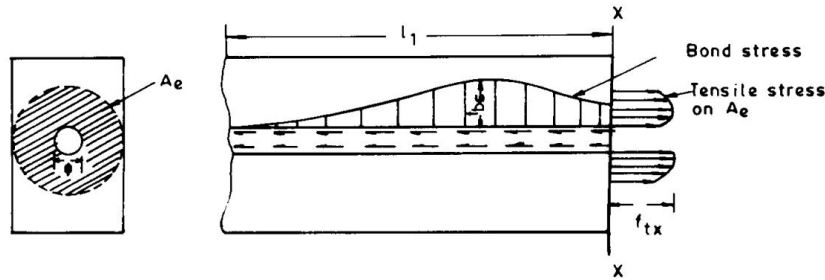


**Fig.1** Distribution of bond stress and axial tensile stress in concrete at a section of distance  $l_1$  from the crack formed in a reinforced concrete member [13].

The general expression derived from this concept is:

$$W_{ma'} = a_m \varepsilon_s F_{rn} \quad (1)$$

- $W_{ma'}$ : maximum crack width
- $a_m$ : average distance between cracks at the instant when the first cracks appear.
- $\varepsilon_s$ : strain of the tensile reinforcement. It is determined by strain compatibility in the cracked section.
- $F_{rn}$ : factor that considers the effect of concrete cover, which is calculated by the ratio  $\frac{h-x}{d_1-x}$ .

Let " $x$ " be the depth of the neutral line of the cracked section, " $h$ " be the total height of the element, and " $d_1$ " be the effective height of the wire or bar closest to the lower end of the rib.

The average crack spacing at the initial stage is calculated by the following expression:

$$a_m = \frac{K_T * f_{ct} * A_e}{K_b * \left(\frac{M_{cr}}{M_n}\right)^Y * f_{bu} * \sum_{i=1}^{i=n} \frac{d_i - x}{d - x} * \pi * \phi_i} \quad (2)$$

- $f_{ct}$ : tensile stress of the mortar.
- $A_e$ : effective tensile area of the mortar.
- $f_{bu}$ : bond stress of the reinforcement.
- $d_i$ : effective height of the bar or wire " $i$ ".
- $d$ : effective height of the element.
- $\phi_i$ : diameter of the bar or wire " $i$ ".
- $K_b$ : empirical factor that considers the distribution of tensile stresses in the effective area.  
 $K_b = 2/3$ .

- $K_T$ : empirical factor that considers the characteristics of the reinforcement surface.  
 $K_T = K_b = 2/3$
- $\gamma$ : empirical factor. Desayi determines in his research that  $\gamma = 0,4$
- $M_{cr}$ : cracking moment of the mortar
- $M_n$ : bending failure moment of the channel slab.

## 2.1 Development of the computational model to predict the bending failure moment of the channel slab.

The results of the tests performed by Desayi and Ganesan [13] are used as a reference for the development of the computational model provided to calculate the failure moment of the target elements under study. These are divided into two groups of three specimens: Elements F1 and F2 are 2,5 m long; F4 and F5 are 3,0 m long; F4 and F5 are 3,5 m. The reinforcement consists of galvanized steel square cell meshes of wires spaced at 6,25mm in both directions, and diameter 0,7 mm; high strength steel plain bars of 6,8 mm and 4 mm; and transverse fences of 4 mm. The modulus of elasticity of the steel meshes is 196 000MPa and yield stress 216MPa, while the modulus of elasticity of the bars is 200 000MPa and yield stress 450MPa.

The difference in each group lies in the distribution of longitudinal reinforcement and spacing of transverse bars, and in all cases, they were reinforced with two meshes (Table 1). For the mortar, a dosage of 1:2:0.43 was used, with a compressive strength of 32,5MPa.

**Table 1.** Details of the reinforcement used in each group of elements tested.

Group	Transverse bars	Longitudinal bars
F1, F4 y F7	@135mm $\varnothing$ 4mm	2 $\varnothing$ 6,8mm y 7 $\varnothing$ 4mm
F2, F5 y F8	@100mm $\varnothing$ 4mm	6 $\varnothing$ 6,8mm y 5 $\varnothing$ 4mm

For the simulation, the Midas FEANX program is used, and the general constitutive model conceived is the distributed crack model developed by Hibbit, with a fixed crack direction approach, due to the simplicity and adequate results in the literature [14, 15]. It is decided to composite the mortar with hexahedral finite elements, based on the positive experiences in previous investigations [6, 16]. For the behavior of the mortar in compression, the constitutive law proposed by Popovics [17] is used satisfactorily by Tian [16], whose expression is:

$$\sigma = f_{cm} \left( \frac{\varepsilon}{\varepsilon_{c1}} \right) \left( \frac{n}{n-1 + \left( \frac{\varepsilon}{\varepsilon_{c1}} \right)^n} \right) \quad (3)$$

- $\sigma$ : compressive stress of mortar
- $f_{cm}$ : compressive strength of mortar
- $\varepsilon$ : compressive strain of the mortar
- $\varepsilon_{c1}$ : compressive strain corresponding to the maximum compressive stress of the mortar.
- $n = 0,058f_{cm} + 1,0$

To represent its tensile behavior, it was decided to use Hordijk's expression [18], a law used by several researchers with excellent results [19-21]. Its expression is shown below:

$$\sigma = f_{ct} \left( 1 + \left( 3 \frac{w}{w_c} \right)^3 \right) \exp \left( -c_2 \frac{w}{w_c} \right) - \frac{w}{w_c} (1 + c_1^3) \exp(-c_2) \quad (4)$$

- $c_1$  and  $c_2$  are empirical factors of values 3 and 6,93, respectively.
- $w_c$ : is the crack width corresponding to tensile stress equal to 0, and is obtained according to the relation:

$$w_c = 5,14 \frac{G_f}{f_{ct}} \quad (5)$$

- $G_f$ : fracture energy of the first tensile mode, calculated by the expression recommended in CEB-FIB model code 1990, for the minimum value indicated  $G_{f0} = 0,025 MPa$  in correspondence to the fineness of the solid compounds of the mixture [16]:

$$G_f = G_{f0} \left( \frac{f_{cm}}{10} \right)^{0,7} \quad (6)$$

The longitudinal and transverse reinforcement are modeled with the embedded bar property, assuming perfect bonding between the reinforcement and the mortar matrix to simplify the analysis. The meshes were modeled as plain stress of equivalent thickness, shaped with rectangular finite elements to reduce computational time [16]. In this study, the reinforcement was defined with elastic behavior up to the yield point and perfectly plastic once the yield point has been reached. The load is assigned with an induced displacement [14] and it is decided to model half of the slab by applying the appropriate constraints to generate the symmetry of a simply supported element (Fig. 2).

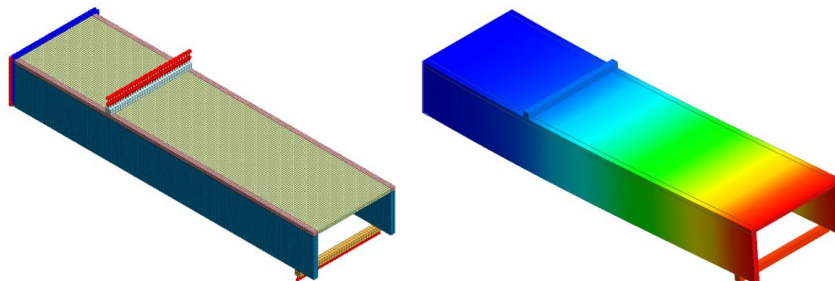


**Fig.2** Computational model developed in Midas FEA NX.

Model calibration is carried out with respect to the failure moment of group 1 elements (F1, F4 and F7). The mesh density of 10 x10 x10 mm was chosen for the hexahedra that simulate the mortar due to its stability and lower computational cost than other denser meshes [16]; and for the linear and surface elements, the sizes of 20 mm and 20 x 20 mm were chosen, respectively. The average failure moment of the group is 12,94 kNm, while that obtained in the simulation was 13,95 kNm, which represents a relative error of 7,8%, so it is decided to use the finite element and mesh density adopted for the modeling.

For the validation, the elements of group 2 (F2, F5 and F8) were chosen, whose average resistant moment is 18,70 kNm. The result of the simulation was 19,64 kNm and its difference with respect to that recorded in the tests is 5%, so it is considered that the model is validated.

## 2.2 Parametric study

The calculation of the maximum crack width involves a group of variables related to the mechanical properties of the mortar and reinforcement, the geometric characteristics of the steel

bars and wire mesh, the dimensions of the element, and the magnitude and manner of load application.

For the analysis, it is assumed as a reference the cross-section of the slab of the Ferrocement Residential Building System (SERF), with a flange width of 400mm, average thickness of 25 mm and total height between 120 mm and 160 mm [1] (Fig 3).

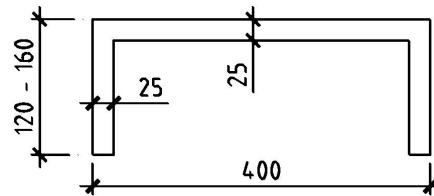


**Fig.3** Cross section of the channel slab to be analyzed.

According to practical design recommendations, the mortar for the project is designed with a compressive strength of 30MPa [1]. For this value, the direct tensile strength is determined as 8% of  $f'_c$  [13], and the flexural strength is estimated from the empirical expression (7), indicated by the American Concrete Institute ACI 318-2019. The Young's modulus of the mortar is assumed as the secant modulus from the origin to  $0.40 f'_c$  of Popovics' constitutive law [16, 17]. The resulting values are shown in Table 2.

$$f_r = 0,62\sqrt{f'_c} \quad (7)$$

Smooth high strength steel bars with similar characteristics to those used by Desayi and Ganesan are chosen for this study, since the value of the empirical factor was validated for this type of surface and its diameter allows the concrete cover to be higher than the minimum standard established in the ACI 318-2019 so that the bar does not fail by adhesion. According to the recommendation of the same research, the bond stress for this type of reinforcement is calculated by the expression (8), from the indication of the British Standard BS 8110-1:1997.

$$f_{bu} = 0,28\sqrt{f'_c} \quad (8)$$

The reinforcement is constituted by a 4mm diameter steel bar at the upper end and a 6mm diameter bar at the lower end of each rib, to comply with the minimum reinforcement area standardized by ACI 318 - 2019. In addition, 4mm transverse steel bars are placed every 135mm to ensure that the elements do not fail by shear (Fig. 4).

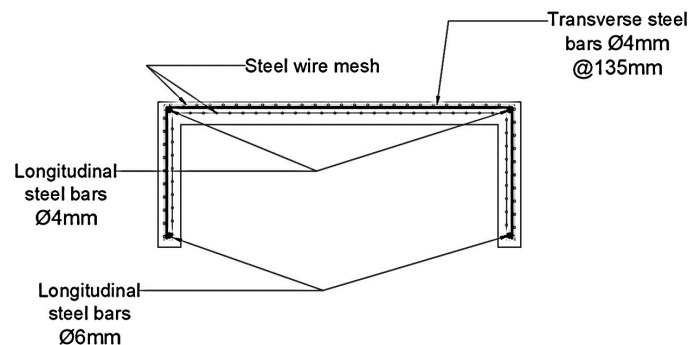


**Fig.4** Slab reinforcement.

To study the influence of the steel wire mesh, a square cell mesh of wire diameter 1mm spaced at 25mm in both directions (@25x25 $\phi$ 1); and another of wire diameter 2mm spaced at 50mm (@50x50 $\phi$ 2) are chosen, as they are two of the most used commercial meshes in the region. Table 2 summarizes the mechanical properties of the materials considered.

**Table 2.** Mechanical properties of channel slab materials

Mechanical properties	Value (MPa)
Compressive strength of mortar $f'_c$	30
Direct tensile strength of mortar $f_{ct}$	2,4
Mortar flexural strength $f_r$	3,4
Deformation modulus of mortar $E_c$	11 810
Bond stress $f_{bu}$	1,5
Yield stress of steel bars $f_{sy}$	450
Deformation modulus of steel bars $E_s$	200 000
Yield stress of steel wire meshes $f_{my}$	304
Deformation modulus of steel meshes $E_m$	190 000

The meshes will be arranged in three variants as shown in Table 3, taking as criteria the specific surface area ( $S_r$ ), defined by the relationship between the total surface area of the reinforcement in contact with the mortar and the volume of the element, and the volume factor ( $V_f$ ), ratio of the volume of the reinforcement to the volume of the element, two recommended factors for the geometric characterization of this type of reinforcement [1]. In addition, an additional variant is foreseen in which this reinforcement is not used. The values defined for the specific surface area and the volume factor are in a range of 0 – 0,20cm<sup>-1</sup> and a range of 0 - 1%, with the purpose of analyzing lower values than those considered for ferrocement, due to the distinctive properties of this material [1].

**Table 3.** Reinforcement variants with galvanized steel wire mesh.

Variant	Nomenclature	$S_r$ (cm <sup>-1</sup> )	$V_f$ (%)
2 meshes @25x25 $\phi$ 1, with 5mm concrete cover.	2@25x25 $\phi$ 1	0,20	0,5
2 meshes @50x50 $\phi$ 2, with 3mm concrete cover	2@50x50 $\phi$ 2	0,20	1,0
1 mesh @50x50 $\phi$ 2, with 3mm concrete cover	1@50x50 $\phi$ 2	0,10	0,5
Without steel wire mesh	WM	0	0

The height is varied in three levels: 120 mm, 140 mm and 160 mm, typical heights in this type of channel slabs, and 3 clear spans are studied: 3,2 m, 3,6 m and 4,0 m, corresponding to the dimensions of the most common spaces in homes. The loads were adopted for a typical load state of a residential floor: service load of 1,5 kN/m<sup>2</sup>, load of self-weight of the slab (depending on the depth) and permanent load of 2,0 kN/m<sup>2</sup>.

In order to evaluate whether the influence of the three factors studied on the maximum value of crack width is significant, a statistical analysis is carried out, with a confidence level of 95%. The multilevel factorial experiment, divided into three independent study variables for a behavior, is summarized in Table 4 below.

**Table 4.** Independent study variables and their corresponding levels.

Independent variables	Levels			
	Total height (mm) h	120	140	160
Clear span (mm) L	3200	3600	4000	-
Reinforcement	2@25x25ø1	2@50x50ø2	1@50x50ø2	WM

The results show that in all cases the influence of the variables studied is significant. As the height and the area of reinforcement increase, the crack opening decreases, but not with the span of the element, where the relationship is directly proportional (Fig. 5a). The order from greatest to least influence is reinforcement variant, slab length and height (Fig. 5b). The interaction between total height and free span, and the interaction between the reinforcement variant and free span also have an influence. The larger the span, the larger the crack width increases because, for the same load state, the acting bending moment increases and with it the deformation of the reinforcing steel. As the reinforcement volume of the mesh and the specific surface area increase, the maximum crack width decreases.

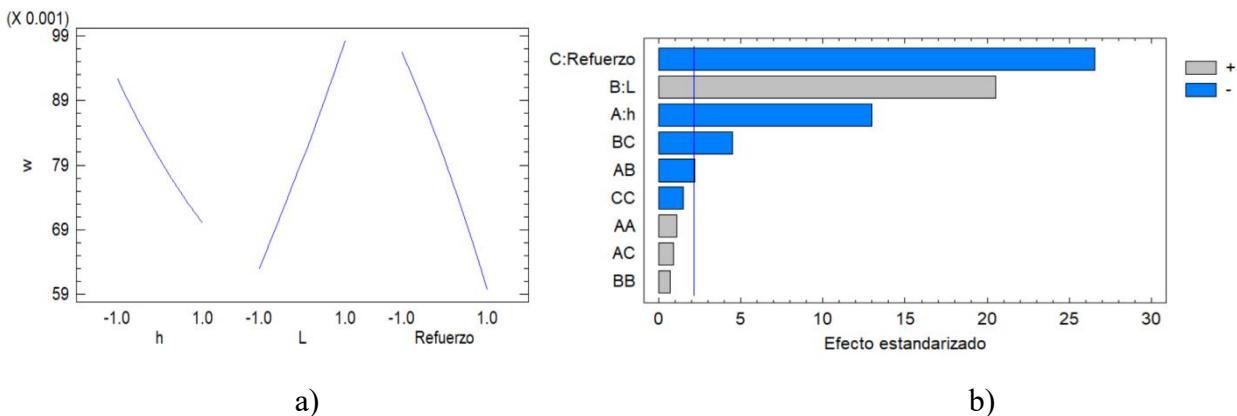


**Fig.5** Statistical results a) Main effects plot for the maximum crack width. b) Standardized Pareto plot for the maximum crack width

### 3. Results

The maximum crack width values for each combination of the designed experiment are shown in Table 5.

**Table 5:** Maximum crack width in reinforced mortar channel slab

Span (mm)	Reinforcement	Crack width (mm)		
		Height (mm)		
		120	140	160
3200	2@25x25ø1	0,071	0,066	Sin grietas
3200	2@50x50ø2	0,057	0,045	Sin grietas
3200	1@50x50ø2	0,087	0,075	Sin grietas
3200	WM	0,152	0,146	Sin grietas
3600	2@25x25ø1	0,090	0,083	0,068
3600	2@50x50ø2	0,073	0,058	0,052
3600	1@50x50ø2	0,111	0,095	0,086
3600	WM	0,193	0,184	0,178
4000	2@25x25ø1	0,111	0,099	0,084

4000	2@50x50ø2	0,090	0,071	0,064
4000	1@50x50ø2	0,136	0,117	0,107
4000	WM	0,238	0,227	0,220

The results show a decrease in the crack width for the slabs studied for those reinforced with 2@50x50 ø2mm (higher reinforcement volume factor). For the same reinforcement volume, slabs with 2@25x25ø1 and 1@50x50ø2, the first variant, with a greater specific surface, controls cracking better. On the other hand, slabs reinforced with 2 meshes of 50x50ø2 have a smaller crack width than those with 2 meshes @25x25ø1, even though they have the same specific surface area. It should be noted that in the case of 160mm slabs with a span of 3200 m, they do not crack even without reinforcing mesh.

Figure 6 shows a graphic comparison of the crack opening values obtained in the analysis with respect to the value established as a limit in the ACI 549 1R-18 standard.

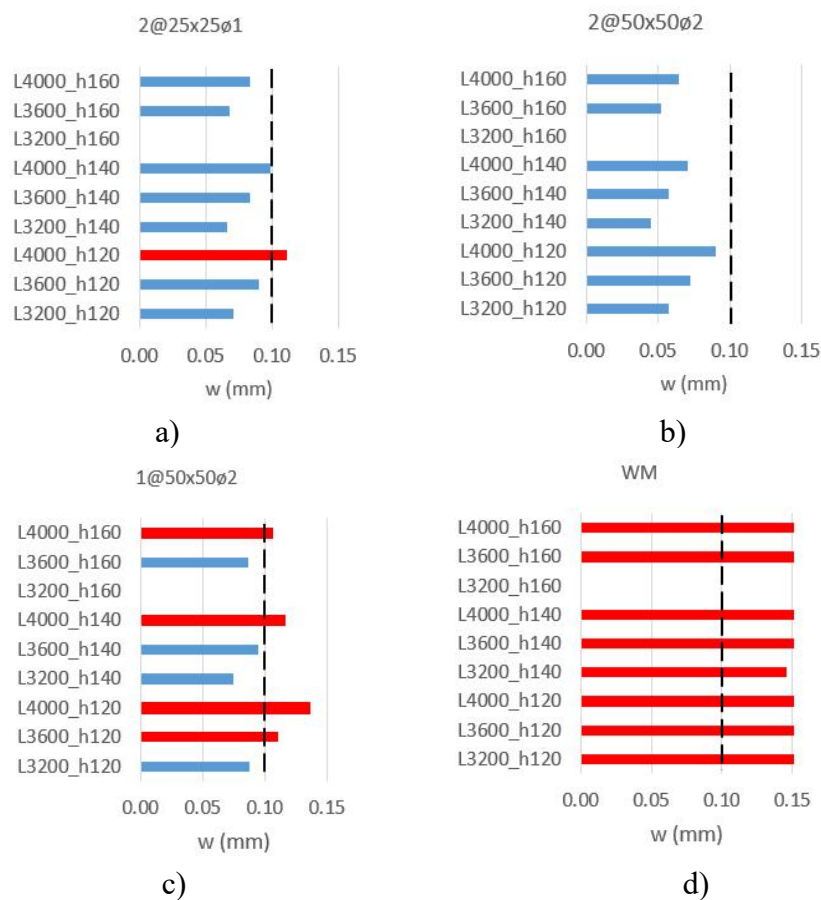


**Fig.6** Maximum crack width. a) Reinforcement variant 2@25x25ø1, b) Reinforcement variant 2@50x50ø2, c) Reinforcement variant 1@50x50ø2, d) No reinforcement mesh. Crack widths smaller than 0,10 mm are shown in blue and those larger than 0,10 mm in red.

Analysis of the graphs shows that elements without galvanized steel mesh do not meet the durability requirements, as they exceed the maximum crack width limit. On the contrary, slabs reinforced with 2 meshes @25x25ø2 guarantee compliance with the crack opening limit state for all the spans and depths studied.

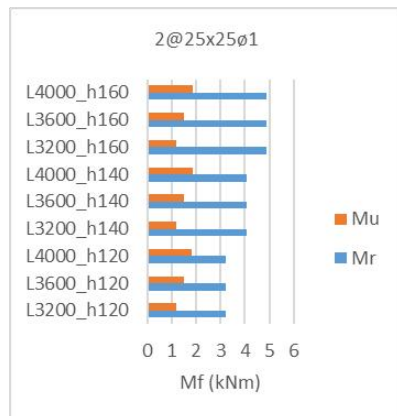
In slabs with 2@25x25ø1 reinforcement, the crack width requirements are met for most of the ranges studied, except for the 120mm height variant in a 4000mm span. With the 1@50x50ø2

variant, the crack widths are less than 0.10 mm for spans equal to or less than 3600 mm, except for the 120mm high panel.

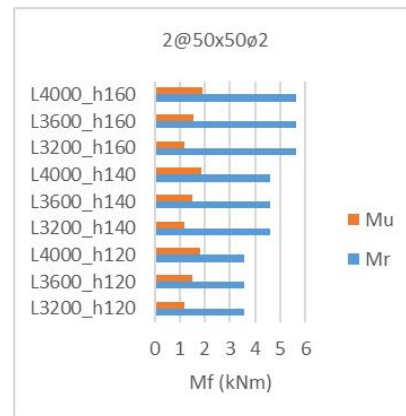
To complement the study, the ultimate limit state in bending is checked to verify the assumption that the elements resist the load considered. The results of the nominal moments obtained from the modeling are shown in Table 6 and in Figure 7, the comparison of the resistant moments ( $M_r$ ) with the estimated acting moments ( $M_u$ ). A safety factor of 0,9 was established, and the critical combination 1,2CP+1,6CU was considered for the calculation of the uniformly distributed load, according to ACI 318-2019.

**Tabla 6:** Nominal or failure moments in reinforced mortar channel slab  
Nominal moment (kNm)

Span (mm)	Reinforcement	Height (mm)		
		120	140	160
3200	2@25x25 $\phi$ 1	3,59	4,52	5,42
3200	2@50x50 $\phi$ 2	3,95	5,10	6,23
3200	1@50x50 $\phi$ 2	3,59	4,53	5,42
3200	WM	3,25	3,95	4,70
3600	2@25x25 $\phi$ 1	3,59	4,52	5,42
3600	2@50x50 $\phi$ 2	3,95	5,10	6,23
3600	1@50x50 $\phi$ 2	3,59	4,53	5,42
3600	WM	3,25	3,95	4,70
4000	2@25x25 $\phi$ 1	3,59	4,52	5,42
4000	2@50x50 $\phi$ 2	3,95	5,10	6,23
4000	1@50x50 $\phi$ 2	3,59	4,53	5,42
4000	WM	3,25	3,95	4,70



a)



b)

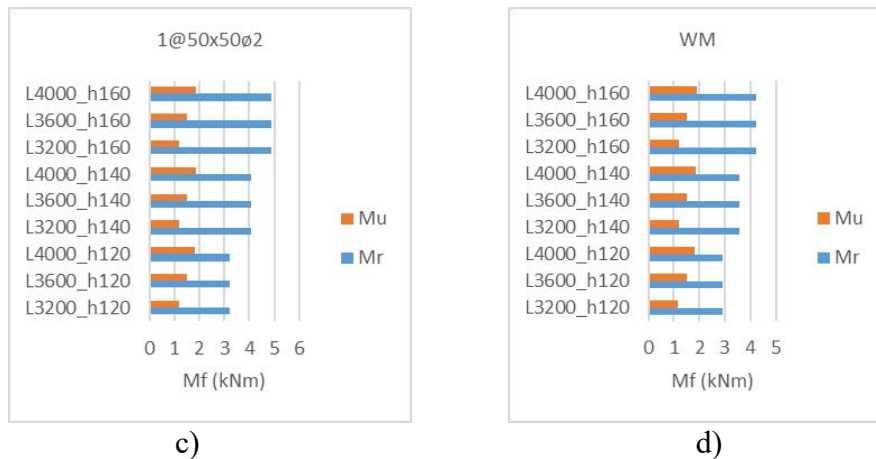


**Fig.7** Comparative graph between resisting moment  $M_r$  and acting moment  $M_u$ . a) Reinforcement variant 2@25x25ø1, b) Reinforcement variant 2@50x50ø2, c) Reinforcement variant 1@50x50ø2, d) Without reinforcement meshes.

The results show that, in all the cases studied, for all the reinforcement arrangements considered, the ultimate bending limit state is met, which confirms that it is the cracking limit state that governs the design of these elements.

#### 4. Conclusions

The cracking in reinforced mortar slabs of channel cross section was studied for conditions of use in residential floors. The results of this research conclude that, in order to ensure the strength and durability criteria established in the design standards:

Reinforced mortar channel slabs, intended to be used as a residential floor solution, cannot be conceived without a galvanized steel wire mesh.

Slabs with a thickness of 120 mm may be used in spans of 3.2 m regardless of the type of reinforcement; to reach 4.0 m, 2 meshes @50x50 and ø2 wires must be placed. Slabs of 140 mm and 160 mm can reach up to 4 m of span with any of the reinforcement configurations studied; in the case of spans of 4 m, a reinforcement greater than 1 mesh @50x50 and ø2 wires must be used.

For channel slabs with main reinforcement consisting of a longitudinal bar at the lower end of each rib, it is recommended that the specific surface area and the volume factor induced by the steel mesh be at least  $0,20 \text{ cm}^{-1}$  and 0,50%, respectively, to ensure the durability of floors with clear spans between 3200 mm and 4000 mm.

#### References

- [1] Wainshtok, H. R., *Ferrocemento. Diseño y construcción*, 4ta ed. Riobamba, Ecuador, 2010. ISBN: 978-9942-03-302-4.
- [2] Ahmad, S. F., Lodi, S. H., & Qureshi, J., *Shear behavior of ferrocement thin webbed sections*. Cement and concrete research, 1995. 25(5), pp. 969-979. DOI: [https://doi.org/10.1016/0008-8846\(95\)00092-Q](https://doi.org/10.1016/0008-8846(95)00092-Q)

- [3] Kridaningrat, BBB, Soehardjono, A., y Nuralinah, D. (). *Identifying the effect of thickness on crack width in one-way reinforced concrete slab structures*. Eastern-European Journal of Enterprise Technologies, 2024. 128 (7). DOI: 10.15587/1729-4061.2024.309874
- [4] García, R., & Caldentey, A. P., *Influence of type of loading (tension or bending) on cracking behaviour of reinforced concrete elements. Experimental study*. Engineering Structures, 2020. 222, 111134. DOI: <https://doi.org/10.1016/j.engstruct.2020.111134>
- [5] Golewski, G. L., *The phenomenon of cracking in cement concretes and reinforced concrete structures: the mechanism of cracks formation, causes of their initiation, types and places of occurrence, and methods of detection—A review*. Buildings, 2023. 13(3), 765. <https://doi.org/10.3390/buildings13030765>
- [6] Gomes, J., Carvalho, R., Sousa, C., Granja, J., Faria, R., Schlicke, D., & Azenha, M., *3D numerical simulation of the cracking behaviour of a RC one-way slab under the combined effect of thermal, shrinkage and external loads*. Engineering Structures, 2020. 212, 110493. DOI: <https://doi.org/10.1016/j.engstruct.2020.110493>
- [7] Kaklauskas, G., Sokolov, A., & Sakalauskas, K., *Strain compliance crack model for RC beams: primary versus secondary cracks*. Engineering Structures, 2023. 281, 115770. DOI: <https://doi.org/10.1016/j.engstruct.2023.115770>
- [8] Kanavaris, F., Coelho, M., Ferreira, N., Azenha, M., & Andrade, C., *A review on the effects of cracking and crack width on corrosion of reinforcement in concrete*. Structural Concrete, 2023. 24(6), pp. 7272-7294. DOI: <https://doi.org/10.1002/suco.202300227>
- [9] Naotunna, C., Samarakoon, S. S. M., & Fosså, K., *Applicability of existing crack controlling criteria for structures with large concrete cover thickness*. Nordic Concrete Research, 2021. 64(1), pp. 69–91. DOI: 10.2478/ncr-2021-0002
- [10] Schlicke, D., Dorfmann, E. M., Fehling, E., & Tue, N. V., *Calculation of maximum crack width for practical design of reinforced concrete*. Civil Engineering Design, 2021. 3(3), pp. 45–61. DOI: <https://doi.org/10.1002/cend.202100004>
- [11] Wlodarczyk, M., Lutomirska, M., & Duc, D. T., *Analytical and Experimental Investigations of Crack width for RC Beams in Bending*. In IOP Conference Series: Materials Science and Engineering, 2019, (Vol. 661, No. 1, p. 012076). IOP Publishing. DOI 10.1088/1757-899X/661/1/012076.
- [12] El Naas, A. A. A., El Hashimy, H. M., & El Kashif, K. F., *Comparative analytical study on crack width of reinforced concrete structures*. Civil Engineering Journal, 2021. 7(07), 1203-1221. DOI: <http://dx.doi.org/10.28991/cej-2021-03091720>.
- [13] Desayi, P., & Ganesan, N., *Determination of maximum crack width in ferrocement flexural elements of channel cross section*. International Journal of Cement Composites and Lightweight Concrete, 1984. 6(3), 169-177. DOI: [https://doi.org/10.1016/0262-5075\(84\)90005-8](https://doi.org/10.1016/0262-5075(84)90005-8)
- [14] Busse, D., & Empelmann, M., *Bending behavior of high-performance, micro-reinforced concrete*. Structural Concrete, 2019. 20(2), 720-729. DOI: <https://doi.org/10.1002/suco.201700246>

- [15] Hibbitt, H. D., *A simplified model for concrete at low confining pressures*. Nuclear engineering and design, 1987. 104(3), 313-320. DOI: [https://doi.org/10.1016/0029-5493\(87\)90209-3](https://doi.org/10.1016/0029-5493(87)90209-3)
- [16] Tian,S., *Shear behaviour of ferrocement deep beams*, Phd, School of mechanical, aerospace and civil engineering, The University of Manchester, 2013.
- [17] Popovics, S. *A numerical approach to the complete stress-strain curve of concrete*. Cement and concrete research, 1973. 3(5), 583-599. DOI: [https://doi.org/10.1016/0008-8846\(73\)90096-3](https://doi.org/10.1016/0008-8846(73)90096-3)
- [18] Hordijk, D. A., *Tensile and tensile fatigue behavior of concrete; experiments, modelling and analyses*. Heron Journal, 1992. 37(1). <http://worldcat.org/issn/00467316>
- [19] Rimkus, A., Cervenka, V., Gribniak, V., & Cervenka, J., *Uncertainty of the smeared crack model applied to RC beams*. Engineering Fracture Mechanics, 2020. 233, 107088. DOI: <https://doi.org/10.1016/j.engfracmech.2020.107088>
- [20] Broo, H., Plos, M., Lundgren, K., & Engström, B., *Simulation of shear-type cracking and failure with non-linear finite-element method*. Magazine of Concrete Research, 2007. 59(9), 673-687. DOI: <https://doi.org/10.1680/mac.2007.59.9.673>
- [21] Díaz, R. A. S., Nova, S. J. S., da Silva, M. C. T., Trautwein, L. M., & de Almeida, L. C., *Reliability analysis of shear strength of reinforced concrete deep beams using NLFEA*. Engineering Structures, 2020. 203, 109760. DOI: <https://doi.org/10.1016/j.engstruct.2019.109760>

### Conflict of Interest

The authors declare no conflict of interest.

### Author's Contributions

Gabriel Martínez Licea. ORCID: <https://orcid.org/0009-0007-9161-9739>  
 Conceptualization, Research and Writing.

Isel del Carmen Díaz Pérez. ORCID: <https://orcid.org/0000-0001-9615-6197>  
 Conceptualization, Supervision and Manuscript Revision.

Hugo Rafael Wainshtok Rivas. ORCID: <https://orcid.org/0000-0001-8849-5682>  
 Conceptualization, Supervision and Manuscript Revision.